J Solid State Electrochem (2014) 18:2193–2200
DOI 10.1007/s10008-014-2462-7

ORIGINAL PAPER

PANI–TiC nanocomposite film for the direct electron transfer of hemoglobin and its application for biosensing

Sai Zhang · Dawei Zhang · Qinglin Sheng · Jianbin Zheng

Received: 3 June 2013 / Revised: 25 January 2014 / Accepted: 13 March 2014 / Published online: 10 April 2014

Abstract A novel polyaniline and titanium carbide (PANI–TiC) nanocomposite was synthesized by an in situ chemical oxidative polymerization method, and a hydrogen peroxide (H_2O_2) biosensor was fabricated by PANI–TiC with hemoglobin (Hb)-modified glassy carbon electrode (GCE). Scanning electron microscope and energy dispersive X-ray spectroscopy showed the morphology and ingredient of PANI–TiC. Electrochemical investigation of the biosensor showed a pair of well-defined, quasi-reversible redox peaks with E_{pa}=−0.318 V and E_{pc}=−0.356 V (vs SCE) in 0.1 M, pH 7.0 sodium phosphate-buffered saline at the scan rate of 150 mV s^{-1}. Transfer rate constant (k_s) was 2.01 s^{-1}. The Hb/PANI–TiC/GCE showed a good electrochemical catalytic response for the reduction of H_2O_2 with the linear range from 0.5 to 285.5 μM and the detection limit of 0.2 μM (S/N=3). The apparent Michaelis–Menten constant (K_m) was estimated to be 1.21 μM. Therefore, the PANI–TiC as a novel matrix opened up a further possibility for study on the design of enzymatic biosensors with potential applications.

Keywords Biosensor · Electrochemical · Hemoglobin · PANI–TiC nanocomposite · Hydrogen peroxide

Introduction

Direct electrochemistry behavior of redox proteins is important for the research of their metabolic processes and construction of biosensors and bioreactors. In recent years, the direct electron transfer (DET) of biologically important proteins has become one of the hottest research areas due to its significance in both theoretical and practical application [1, 2]. Heme-based proteins such as hemoglobin (Hb), myoglobin (Mb), horseradish peroxidase (HRP), and cytochrome c (Cyt c) have been investigated. Among those proteins, Hb is generally used as a model for the DET process between redox proteins and the modified electrode in the biological systems, due to the advantages of commercial availability, well-documented structure, and excellent electrocatalytic abilities. However, the DET between proteins and bare solid electrode is difficult because the electroactive centers of proteins are deeply embedded in its structure, as well as adsorptive denaturation and unfavorable orientations of proteins onto electrode surfaces [3–5]. Hence, different biocompatible immobilizing materials, including polymer [6–8] and nanomaterials [9–17], are used to promote the DET.

Immobilization of redox proteins is a significant step in constructing biosensors or bioreactors [18]. Biocompatible materials have been used widely by entrapment or encapsulation of an enzyme or protein within them to realize direct electrochemistry of redox proteins for their desirable properties, such as nontoxic, biocompatible, and potential applications for the fabrication of biosensors [19]. For example, Åsberg et al. have utilized a highly conducting poly(3,4-ethylenedioxythiophene)/poly(styrenesulfonate) aqueous dispersion to build a conducting hydrogel matrix [20]. Pan et al. have reported the synthesis of multifunctional polyaniline (PANI) hydrogel with high surface area and three-dimensional porous nanostructures, which exhibited excellent electronic conductivity and electrochemical properties [21]. Zhai et al. have also fabricated a highly sensitive glucose enzyme sensor based on PtNPs-PANI hydrogel heterostructures [22]. Polymer nanocomposites through a small amount of polymer matrix are scattered with nanometer-sized packing particles, such as together, inside the ester/layer has clay nanocomposite materials. Because nanoparticles have some special properties such as the nanometer-scale effect, large-specific surface area, volume effect, and

S. Zhang · D. Zhang · Q. Sheng · J. Zheng (✉)
Institute of Analytical Science/Shaanxi Provincial Key Laboratory of Electroanalytical Chemistry, Northwest University, Xi'an 710069, Shaanxi, China
e-mail: zhengjb@nwu.edu.cn

polymer matrix strong interface interaction, which make polymer nanocomposites improved in mechanic and thermodynamic properties. PANI is one of the most important conducting polymers due to its ease of synthesis at low cost, good process ability, high polymerization yield, high conductivity, good redox reversibility, and environmental stability. It has a wide range of applications for super capacitors [23, 24], fuel cells [25], electrocatalysis [26], biosensors [27], etc. TiC is typical of transition metal carbide. Its key type is held together by ionic bond, covalent bond, and metallic bond. Nano-TiC has many advantages like high purity, small size, distribution uniformity, specific surface area, and high surface activity. And, it exhibits high electrical conductivity, low density, and catalytic activity. The TiC is also widely applied, such as biosensors [28], the methanol electrooxidation applications [29], supercapacitor [30], direct fuel cells [31, 32], thermal stability [33], Li-ion batteries [34], and energy-related applications [35]. Those research data above about PANI and TiC provide favorable conditions for enzyme or protein immobilization.

In this work, we prepare the novel PANI–TiC nanocomposite by the in situ chemical oxidative polymerization method. And, we describe the direct electrochemistry of Hb immobilized on PANI–TiC composite matrix. The electrochemical behaviors of the composite film are thoroughly investigated by cyclic voltammetry and electrochemical impedance spectroscopy. The resulting biosensor can catalyze the reduction of hydrogen peroxide (H_2O_2). Accordingly, the PANI–TiC composite matrix can be applied as a useful material for the design of enzymatic biosensors and bioelectronics based on bioelectrochemistry.

Experimental

Reagents

Bovine hemoglobin (Hb, MW 67000) was from Sigma (St. Louis, USA) and used without further purification. TiC powders (>99 % purity, 40 nm in diameter) were purchased from Kaiser Company (China). Aniline (Beijing Chemical Co.) was distilled under reduced pressure. A 0.1 M sodium phosphate-buffered saline (PBS) with various pH values was prepared by mixing stock standard solutions of Na_2HPO_4 and KH_2PO_4 and adjusting the pH value with 0.1 M H_3PO_4 or NaOH. The solution of Hb was prepared in 0.1 M PBS (pH 7.0) just before each experiment. Other reagents were of analytical reagent grade, and double-distilled water was used in all the experiments.

Apparatus

Cyclic voltammetry (CV) and electrochemical impedance spectroscopy (EIS) were carried out on a CHI 660D electrochemical workstation (Shanghai CH Instrument Co., Ltd., China). A traditional three-electrode system was used with an Hb-modified electrode as working electrode, a platinum wire as auxiliary electrode, and a saturated calomel electrode (SCE) as reference electrode. Thus, all the potentials reported in this work had been measured versus SCE reference electrode. The rotating disk electrode voltammograms were performed on a glassy carbon rotating disk electrode (3.0 mm diameter, Princeton Applied Research) with a motor-controlled rotor (Princeton Applied Research). Scanning electron microscopy (SEM) was done with a JSM-6700 F scanning electron microscope (Japan Electron Company, Japan). Transmission electron microscopy (TEM) images were acquired with a JEOL JEM-3010 high-resolution transmission electron microscope using an accelerating voltage of 150 kV. All the tested solutions were purged with highly purified nitrogen for at least 20 min prior to a series of voltammetric experiments and maintained under nitrogen atmosphere during the measurements. All the electrochemical experiments were conducted at room temperature (25±2 °C).

Preparation of the PANI–TiC

PANI–TiC nanocomposite was prepared as follows: A certain amount of cetyltrimethylammonium bromide (CTAB) was dissolved in 250-mL double-distilled water; then, 0.60-g TiC powder was added with stirring for 1 h, after which, 0.66-g oxalic acid was added. After 10-min stirring, 2.86 g ammonium persulfate dissolved in 20-mL solution was added to the mixture. At last, 0.90 mL aniline was added to the above mixture and maintained the system at 0 to 10 °C for 24 h. Finally, the as-prepared PANI–TiC was washed with double-distilled water and ethanol and dried in vacuum oven at 60 °C for 24 h.

Preparation of the modified GCE

GCE of 3-mm diameter, before use, was first polished to a mirror-like with 1.0, 0.3, and 0.05 mm Al_2O_3 slurry on a polish cloth and rinsed with double-distilled water, and then sonicated in ethanol and double-distilled water for 5 min, respectively. A traditional three-electrode system was used with modified electrode as working electrode, a platinum wire as auxiliary electrode, and a SCE as reference electrode. Thus, all the potentials reported in this work had been measured versus SCE reference electrode. Ten milligrams of PANI–TiC and 1 mL of double-distilled water were mixed, and then, to use ultrasound makes material scattered evenly. And, 40 μL of 20 mg/mL Hb was added, shaking in a rocking incubator at 37 ±0.2 °C mixed for 24 h, and then, 10 μL of the mixture was cast onto the surface of the bare GCE using a syringe to prepare Hb/PANI–TiC/GCE. For comparison, Hb/GCE and PANI–TiC/GCE were prepared under the same condition. Without use, the modified electrode was stored at 4 °C in a refrigerator.

Results and discussion

Characterization of the PANI–TiC and the Hb/PANI–TiC/GCE

The morphology, size, and the status of agglomeration of the samples were analyzed by SEM. As shown in Fig. 1a, the structure of PANI–TiC consisted of film flake and that of the whole looks like coral reefs' shape. TEM image of the PANI–TiC showed a cubic structure of the TiC and a composite structure of the PANI–TiC (Fig. 1b). Furthermore, the EDS (Fig. 1c) certified strongly that the materials were composed of C, Ti, and N.

EIS is an effective method of probing the features of surface-modified electrodes, which provide useful information on the impedance changes of the electrode surface during the fabrication process [36, 37]. The respective semicircle diameters at the high frequencies corresponded to the charge transfer resistance (R_{ct}) at the electrode surface. Thus, the charge transfer resistance was used as a sensor signal. R_s is the electrolyte solution resistance and R_p is the polarization resistance. R_p obtained at zero potential is described as surface charge resistance (R_{ct}). C_d can be calculated from the frequency associated with maximum $Z''(\omega)$ and R_{ct}. The EIS results of different electrodes are described in Fig. 2. The semicircle of the PANI–TiC/GCE (b) was obviously smaller than that of the Hb/PANI–TiC/GCE (c) and Hb/GCE (d). It meant that the use of the PANI–TiC in the modified electrode provided excellent binder between the electrode and electrolyte, leading to the promotion of the electron transfer rate. The presence of Hb led to the increase of the impedance of the Hb/PANI–TiC/GCE than that of the PANI–TiC/GCE but smaller than that of the Hb/GCE. It further indicated that Hb was effectively immobilized in the composite film and further increased the thickness of the composite film. Inset of Fig. 2 was the equivalent electrical circuit used for fitting the obtained impedance spectra.

In N_2-saturated 0.1 M PBS (pH 7.0), the bare GCE had no peaks (shown in Fig. 3, curve a). The Hb/GCE (curve c) only showed one cathode peak at −0.337 V due to the unstable electron transfer. When adding the PANI–TiC-modified GCE, the Hb/PANI–TiC/GCE (curve d) obviously showed a pair of symmetric redox peaks, which was attributed to the redox process of heme Fe(III)/Fe(II) couple. The above electrochemical performance of different electrodes indicated that PANI–TiC could provide a favorable microenvironment for Hb to retain its natural structure and to realize its direct electrochemistry. PANI–TiC played important roles to facilitate the electron transfer from Hb the synergistic effect of Hb/PANI–TiC which was useful to amplify the signal output.

Direct electrochemistry of Hb/PANI–TiC/GCE

The direct electrochemistry of Hb in the Hb/PANI–TiC/GCE was studied by CV. Cyclic voltammograms (CVs) of Hb at the Hb/PANI–TiC/GCE with different scan rates are shown in Fig. 4. The modified electrode showed a pair of well-defined, quasi-reversible redox peaks with E_{pa}=−0.318 V and E_{pc}=−0.356 V (vs SCE) in PBS (0.1 M, pH 7.0) with the formal potential $E^{0'}$=−0.337 V. The peak-to-peak separation ΔE_p was 38 mV and about 1 ratio of cathodic to anodic current intensity at the scan rate of 150 mV s^{-1}, indicating that the DET for Hb-Fe(III)/Fe(II) was nearly reversible. The redox process of Hb at the Hb/PANI–TiC/GCE gave roughly symmetric anodic and cathodic peaks at relative slow scan rates. When the scan rate increased, the redox potentials (E_{pa} and E_{pc}) of Hb hardly shift. Meanwhile, the redox peak current changed linearly (inset, Fig. 4): $I_{pa}=0.018-7.1\times10^{-3}v$, r=0.9989; $I_{pc}=0.91+8.0\times10^{-3}v$, r=0.9993. This indicated that the electron transfer process for Hb at the Hb/PANI–TiC/GCE was a surface-confined mechanism in the above-mentioned potential scope, manifesting the characteristics of thin-layer surface-controlled electrochemical process.

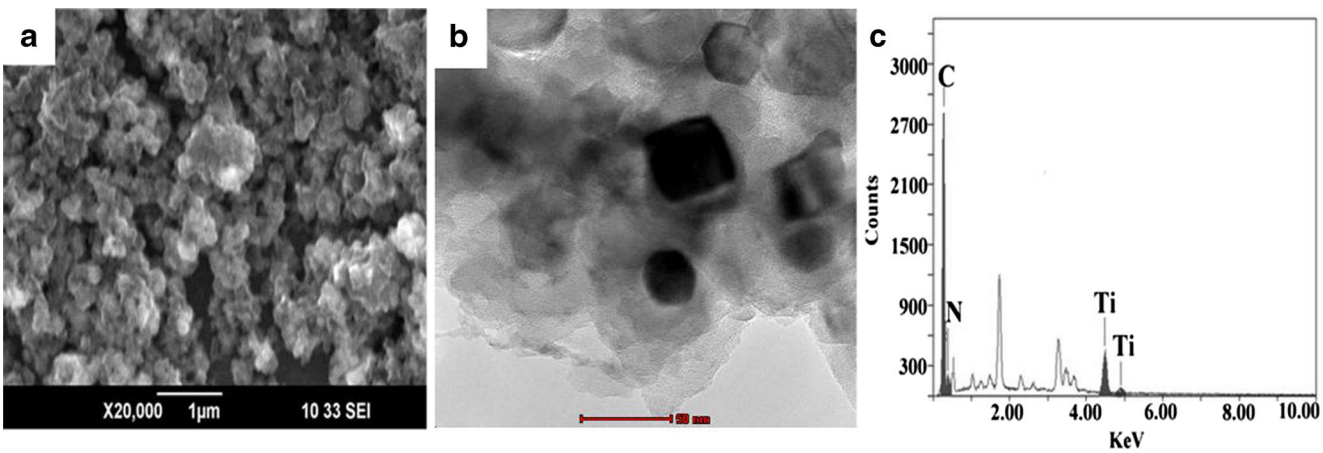

Fig. 1 **a** SEM and **b** TEM images and **c** EDS of PANI–TiC

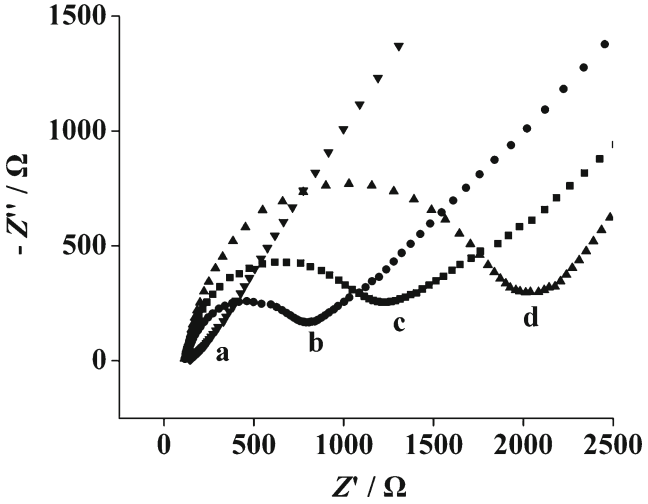

Fig. 2 EIS plots for the bare GCE (*a*), Hb/GCE (*b*), PANI–TiC/GCE (*c*), and Hb/PANI–TiC/GCE (*d*) in a solution of 1 mM $[Fe(CN)_6]^{3-/4-}$+ 0.1 mol/L KCl as the supporting electrolyte. The frequencies swept from 10^5 to 10^{-2} Hz. *Inset* shows the equivalent electrical circuit used for fitting the impedance spectra

The anodic and cathodic peak potentials were linearly dependent on the logarithm of the scan rates (*n*) with slopes of $-2.3RT/\alpha nF$ and $2.3RT/(1-\alpha)nF$, respectively. Hence, the charge transfer coefficient α was calculated as 0.53. Heterogeneous electron transfer rate constant (k_s) was further estimated according to the following equation [38]:

$$\log k_s = \alpha\log(1-\alpha) + (1-\alpha)\log\alpha - \log(RT/nFv) - (1-\alpha)\alpha F\Delta E_p/(2.3RT) \quad (1)$$

where α is the charge transfer coefficient and *n* is the number of electron transfer. *R*, *T*, and *F* symbols have their conventional meanings. ΔE_p is the peak-to-peak potential separation.

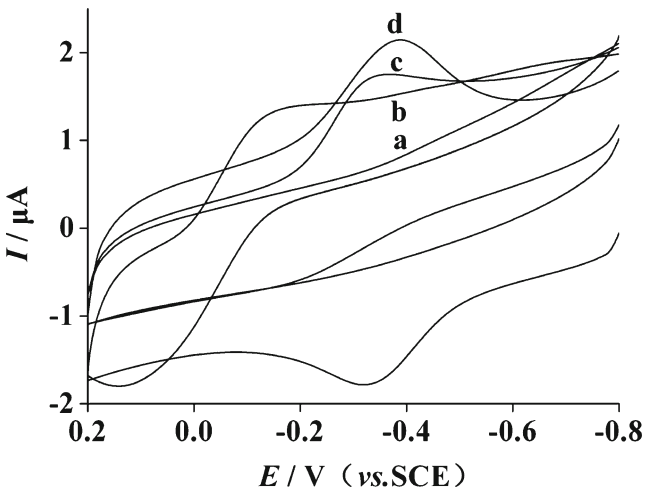

Fig. 3 CVs of the bare GCE (*a*), PANI–TiC/GCE (*b*), Hb/GCE (*c*), and Hb/PANI–TiC/GCE (*d*) in N_2-saturated PBS at the scan rate of 150 mV s^{-1}

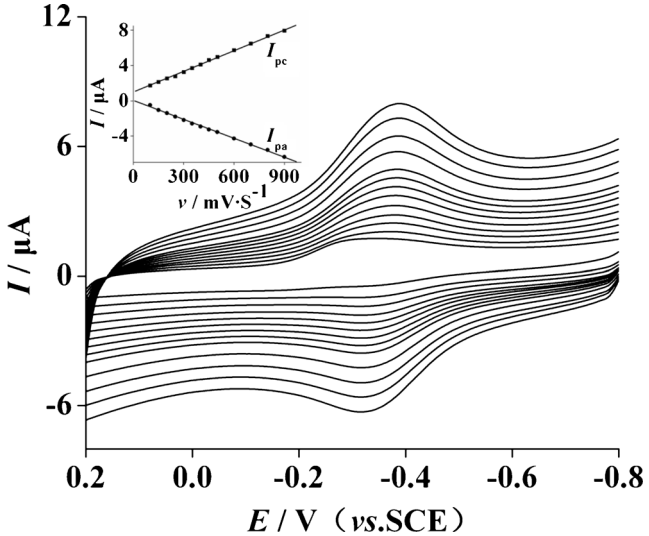

Fig. 4 CVs of the Hb/PANI–TiC/GCE in N_2-saturated PBS with different scan rates (from 100, 150, 200, 250, 300, 350, 400, 450, 500, 600, 700, 800, and 900 mV s^{-1}). *Inset* shows the relationship between cathodic and anodic peak currents with scan rate *v*

As known, k_s reflects the local microenvironment of the Hb immobilized on the electrode. The value obtained here is for typical surface-controlled quasi-reversible electron transfer processes. It neglects rate limiting ion entry or ejection, electron self-exchange, and molecular interactions within the films. Thus, k_s obtained by this method is probably best interpreted as a measure of the rate of the overall electron transfer process dependent on film and electrode properties. The model used here was based on the Butler–Volmer equations [39] for diffusionless and thin-layer-controlled system. The result was 2.01 s^{-1}, which was higher than that 0.332 s^{-1} of the Nafion/Mb/multiwalled carbon nanotubes/carbon ionic liquid electrode (CILE) [40], 1.34 s^{-1} of silk fibroin [41], and 1.02 s^{-1} of DNA/CILE [42]. To compare the electron transfer rate of Hb, the kinetic constant for DET was also calculated from rotating disk electrode experiments. The calculated value of k_s was 2.6 s^{-1}, which was close to the results obtained from the CV experiments. Thus, the PANI–TiC could provide a favorable environment for Hb to undergo a facile electron transfer reaction, which might pave the way for elucidating the relationship between the heme protein structures and biological functions.

Effect of pH values on the DET

The effect of pH values of the solution on the DET of the Hb/PANI–TiC/GCE was investigated (Fig. 5). Results showed that an increase of pH value of the solution from pH 4.0 to 9.0 led to a negative shift of both reduction and oxidation peak potentials of the Hb/PANI–TiC/GCE. By comparison, a better electrochemical response of the immobilized Hb was obtained at pH 7.0. This was contributed to that neutral pH value that

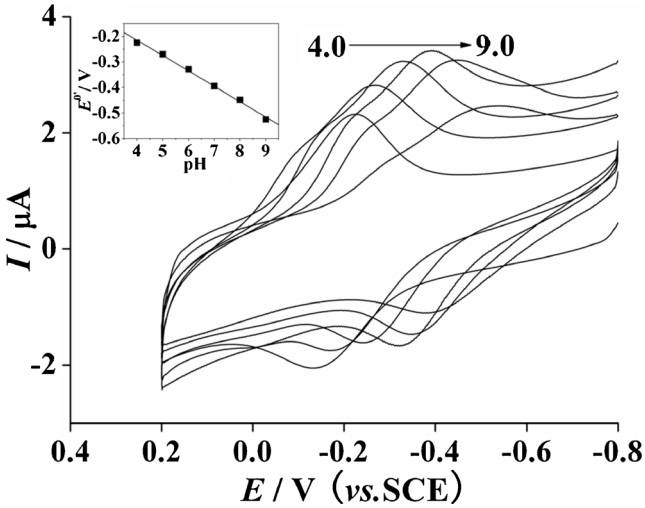

Fig. 5 Influence of the pH value on the CVs of the Hb/PANI–TiC/GCE, pH values (from *left* to *right*) 4.0, 5.0, 6.0, 7.0, 8.0, and 9.0. *Inset* shows the relationship between $E^{0'}$ and pH

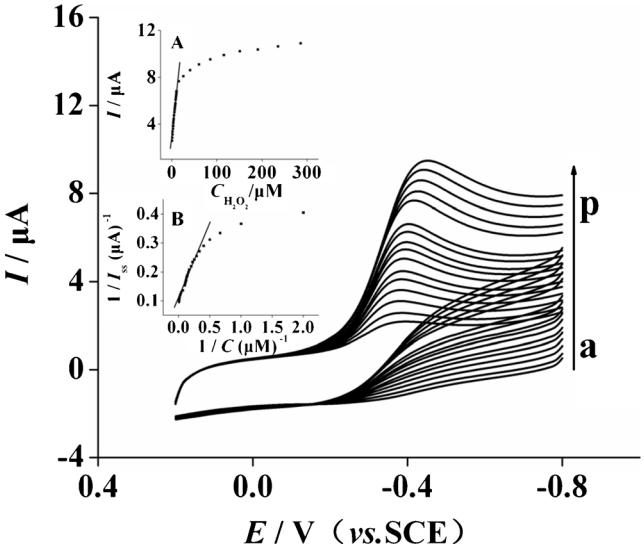

Fig. 6 CVs of the Hb/PANI–TiC/GCE in N_2-saturated PBS with different concentration of H_2O_2 (from *a* to *p*, 0 to 235.5 μM), respectively. *Inset A* shows the linear relationship of I_{pc} and H_2O_2 concentration. *Inset B* shows the determination of the apparent Michaelis–Menten constant

was close to the physiological environment and could retain activity of the Hb effectively. Thus, all the experiments were performed in pH 7.0 PBS unless specially stated. In general, all changes in the peak potentials and currents with the solution pH value were reversible in the pH value range from 4.0 to 9.0. That was, the same CVs could be obtained if the electrode was transferred from a solution with a different pH value to its original solution. The formal potential $E^{0'}$ had a linear relationship with pH values. The linear regression equation was obtained as $E^{0'}$ (mV)=24.2−60.0 pH (n=6, r=0.9977). The shift of $E^{0'}$ depending on the pH value suggested that the redox reaction took place accompanied by the transfer of proton. The slope (−60.0 mV pH^{-1}) was close to that expected theoretically −59 mV pH^{-1} for a one-electron, one-proton reaction [43], indicating that a single proton transfer was accompanied in the electrochemical process of Hb. The electrochemical reduction of Hb could be simply expressed as follows:

$$\mathrm{Hb}\left[\mathrm{heme}\left(\mathrm{Fe^{III}}\right)\right] + \mathrm{e^-} + \mathrm{H^+} \leftrightarrows \mathrm{Hb}\left[\mathrm{H^+}-\mathrm{heme}\left(\mathrm{Fe^{II}}\right)\right] \quad (2)$$

Electrocatalytic ability of the Hb/PANI–TiC/GCE

It is well known that proteins containing heme groups, such as Hb, Mb, and HRP, were able to reduce H_2O_2 electrocatalytically [44–47]. As shown in Fig. 6, the Hb/PANI–TiC/GCE exhibited good catalytic activity toward H_2O_2. When H_2O_2 was added into PBS (0.1 M, pH 7.0), the catalytic reduction peak current at −0.370 V (curve a) increased (curve b–p). Meanwhile, the oxidation peak current of Hb was decreased. The possible mechanism of electrocatalytic reduction of H_2O_2 at Hb-based enzyme electrode could be expressed as follows (Compound I, denoted by $\mathrm{Hb[heme(Fe^{IV})O\cdot^+]}$):

$$\mathrm{Hb}\left[\mathrm{heme}\left(\mathrm{Fe^{III}}\right)\right] + \mathrm{H_2O_2} \leftrightarrows \mathrm{Compound\ I} + \mathrm{H_2O} \quad (3)$$

$$\mathrm{Compound\ I} + \mathrm{H_2O_2} \leftrightarrows \mathrm{Hb}\left[\mathrm{heme}\left(\mathrm{Fe^{III}}\right)\right] + \mathrm{H_2O} + \mathrm{O_2} \quad (4)$$

$$\mathrm{Hb}\left[\mathrm{heme}\left(\mathrm{Fe^{III}}\right)\right] + \mathrm{H^+} + \mathrm{e^-} \leftrightarrows \mathrm{Hb}\left[\mathrm{heme}\left(\mathrm{Fe^{II}}\right)\right] \text{ at electrode} \quad (5)$$

$$\mathrm{Hb}\left[\mathrm{heme}\left(\mathrm{Fe^{II}}\right)\right] + \mathrm{O_2} \leftrightarrows \mathrm{Hb}\left[\mathrm{heme}\left(\mathrm{Fe^{II}}\right)\right]-\mathrm{O_2}\,\mathrm{fast} \quad (6)$$

$$\mathrm{Hb}\left[\mathrm{heme}\left(\mathrm{Fe^{II}}\right)\right]-\mathrm{O_2} + \mathrm{H^+} + \mathrm{e^-} \leftrightarrows \mathrm{Hb}\left[\mathrm{heme}\left(\mathrm{Fe^{III}}\right)\right] + \mathrm{H_2O_2}\,\mathrm{at\ electrode} \quad (7)$$

The overall reaction of Eqs. (2)-(6) would be as follows:

$$\mathrm{H_2O_2} + 2\mathrm{H} + 2\mathrm{e^-} \leftrightarrows 2\mathrm{H_2O} \quad (8)$$

The cathodic peak current had a linear relationship with the concentration of H_2O_2 in the range between 0.5~285.5 μM, as shown in the insert A of Fig. 6, which indicated that the Hb/PANI–TiC/GCE can be used for the detection of H_2O_2. And, the linear regression equation was I_{ss} (μA)=0.414C (μM)+2.55, with a correlation coefficient 0.9983 (n=20). The detection limit was estimated to be 0.2 μM at a signal-to-noise ratio of 3. According to Michaelis − Menten kinetic mechanism, the apparent Michaelis–Menten constant K_m could be

obtained from the electrochemical version of the Lineweaver–Burk equation [48, 49]:

$$1/I_{ss} = 1/I_{max} + K_m/(I_{max}C) \quad (9)$$

Here, I_{ss} is the diffusion limiting current after the addition of the substrate. C is the bulk concentration of the substrate, and I_{max} is the maximum current measured under the saturate substrate conditions. The value of K_m and I_{max} can be obtained by the slope and the intercept of the plot of the reciprocals of the steady-state current versus H_2O_2 concentration. The apparent Michaelis − Menten constant K_m value was calculated to be 1.21 μM, which was much lower than some previous reports [50–58]. It is well known that low value of K_m represents a higher biological affinity of Hb in the catalytic reaction of H_2O_2. And, Hb can retain higher activity in the Hb/PANI–TiC.

In the case where reduction of H_2O_2 at the Hb/PANI–TiC/GCE surface is controlled solely by mass transfer in the solution, the relationship between the limiting current and rotating speed should obey the Levich equation [59]:

$$I_L = 0.620\, nFAD^{2/3}\, v^{-1/6}\, \omega^{1/2} C \quad (10)$$

where D/cm^2 s^{-1}, v/cm^2 s^{-1}, ω/rad s^{-1}, and C/mol cm^{-3} are the diffusion coefficient, the kinematics viscosity, the rotation speed, and the bulk concentration of the reactant in the solution, respectively, and all other parameters have their conventional meanings. The rotating disk electrode voltammograms exhibited an increase in current with increasing rate of rotation (Fig. 7a). Based on Eq. (10), the plot of limiting current I_L as a function $\omega^{1/2}$ should be a straight line. According to the Levich plot (Fig. 7b), the current increases with increasing electrode rotation speed. For an irreversible reaction, the relation between the limiting current and rotating speed has been given by the Koutecky–Levich equation [59]:

$$I^{-1} = I_{kin}{}^{-1} + I_L{}^{-1} \quad (11)$$

where I_{kin}=$nFkC$. It can be seen that the intercepts of all linear plots are positive, clearly indicating the kinetic limitations of the electrode process. Considering that the oxidation of the H_2O_2 substrate is the rate-determining step, the Koutecky–Levich relation was used to construct the plot displayed in Fig. 7c from which the rate constant, k_f, was calculated as 1.4×10^4 M^{-1} s^{-1}.

Stability and reproducibility of the composite-film-modified electrode

The stability of the Hb/PANI–TiC composite-film-modified electrode was first evaluated by examining the cyclic voltammetric peak currents of Hb after continuously scanning for 50 cycles. No decrease of the voltammetric response was

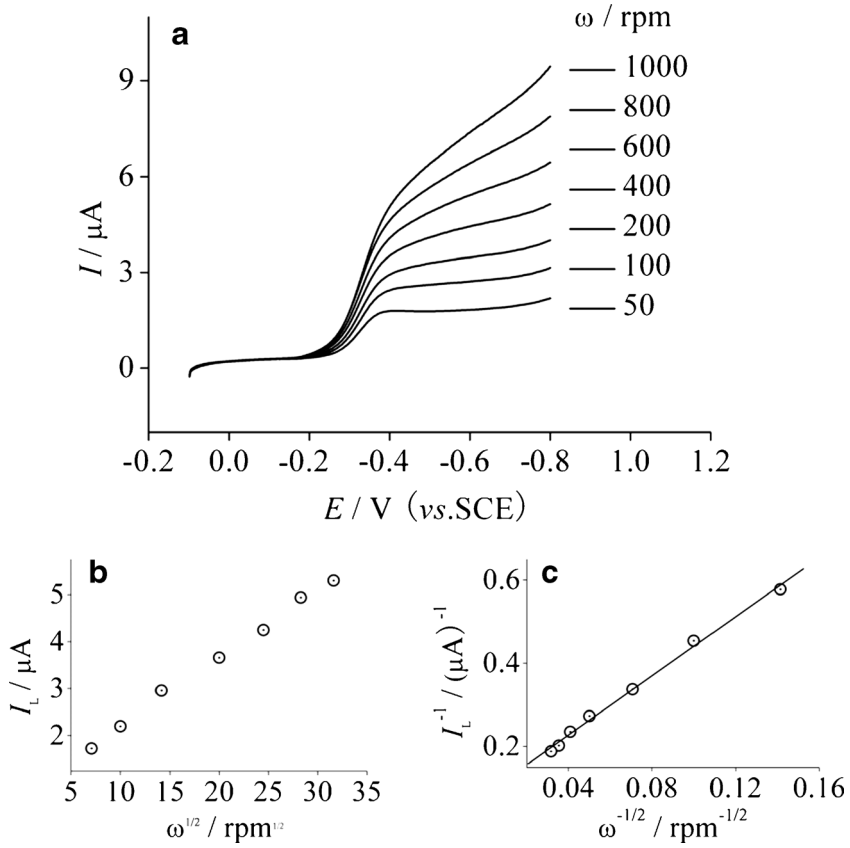

Fig. 7 **a** Rotating disk electrode voltammograms at 100 mV s^{-1} of the Hb/PANI–TiC/GCE in 0.1 M PBS (pH 7.0) containing 0.2 mM H_2O_2. Levich (**b**) and Koutecky–Levich (**c**) plots at −0.40 V for the H_2O_2 reduction reaction

observed, indicating that the Hb/PANI–TiC composite-film-modified electrode was stable in buffer solution. The stability of the composite-film-modified electrode was also checked by measuring the current response of the Hb/PANI–TiC composite-film-modified electrode daily over a period of 30 days. When not in use, the electrode was stored dry at 4 °C in a refrigerator. It was found that the composite-film-modified electrode maintain its 92 % initial activity after 30 days. Conversely, without the presence of PANI–TiC, the current response of the Hb-modified electrode decreased dramatically and maintains its 65 % initial activity after 7 days, after which, the composite film was easily collapsed and falls off from electrode surface. The above results indicated that the PANI–TiC could greatly improve the composite film stably attached on the GCE surface. The repeatability and reproducibility of the biosensor were determined. The repeatability of one electrode was conducted by adding 100 μL of 1.0 mM H_2O_2 into 20 mL of 0.1 M PBS. The relative standard deviation was 3.2 % for six successive assays. Five Hb/PANI–TiC/GCEs prepared by following the identical steps were used to estimate the reproducibility of the biosensor by measuring the current responses of the Hb/PANI–TiC/GCEs to 5.0 μM H_2O_2. The relative standard deviation was 4.9 %.

H_2O_2 may be used as a preservative or decolorant in food industry and additive in production of cosmetic. The sufficient sterilization is considered at 0.03 % H_2O_2 in milk and 0.08 % in bean products. Moreover, the leftover amount did not inspect. The determination of H_2O_2 in milk sample was performed on the sensor utilizing standard addition method. After the current response was determined in 5.0 mL of 0.1 M pH 7.0 PBS containing sample of 500 μL, 40.0 μM of H_2O_2 solutions was successively added to the system for standard addition determination. The concentration of H_2O_2 in milk sample was found to be 1.25×10^{-3} mg mL^{-1} (n=5).

Conclusions

In the present work, we successfully prepared PANI–TiC nanocomposite by the in situ chemical oxidative polymerization method. And, the direct electrochemistry of Hb fabricated using a composite matrix based on PANI–TiC was achieved with a larger electron transfer rate constant of 2.01 s^{-1}. Compared with the absence of PANI–TiC used to fabricate the biosensor, the presence of PANI–TiC accelerated the DET rate between Hb and the substrate electrode significantly. The resulting biosensor showed excellent electrocatalytic activity toward the reduction of H_2O_2 with a wider linearity range and a lower detection limits. The excellent performances of the resulting biosensor might be that the PANI–TiC substantially improved the protein stability. The synergistic effects of Hb/PANI–TiC not only improved the electron transfer ability of our system but also exhibited the signal amplification of nanosize materials. The promising feature of the biocompatible hybrid materials could serve as a versatile platform for the fabrication of electrochemical biosensors.

Acknowledgments The authors gratefully acknowledge the financial support of this project by the National Science Foundation of China (No. 21275116), the Specialized Research Fund for the Doctoral Program of Higher Education of China (No. 20126101120023), the Natural Science Foundation of Shaanxi Province, China (Nos. 2012JQ2010 and 2012JM2013), and the Foundation of Shaanxi Province Educational Committee of China (12JK0576).

References

1. Brajter-Toth A, Chambers JQ (2002) Marcel Dekker, New York
2. Gooding JJ, Wibowo R, Liu J, Yang W, Losic D, Orbons S, Mearns FJ, Shapter JG, Hibbert DB (2003) J Am Chem Soc 125:9006–9007
3. Li WM, Shi Z, Li N, Gu Z (2002) Anal Chem 74:1993–1997
4. Sun W, Li XQ, Wang Y, Zhao RJ, Jiao K (2009) Electrochim Acta 54:4141–4148
5. Feng JJ, Xu JJ, Chen HY (2005) J Electroanal Chem 585:44–50
6. Miscoria SA, Barrera GD, Rivas GA (2006) Sens Actuators B 115: 205–211
7. Retama JR, Lopez-Ruiz B, Lopez-Cabarcos E (2003) Biomaterials 24:2965–2973
8. Yang MH, Yang YH, Liu B, Shen GL, Yu RQ (2004) Sens Actuators B 101:269
9. Baughman RH, Zakhidov AA, De Heer WA (2002) Science 297: 787–792
10. Cai CX, Chen J (2004) Anal Biochem 332:75–83
11. Davis JJ, Coles RJ, Hill HAO (1997) J Electroanal Chem 440:279–282
12. Sun YY, Yan F, Yang WS, Sun CQ (2006) Biomaterials 27:4042–4049
13. Salimi A, Sharifi E, Noorbakhsh A, Soltanian S (2007) Biosens Bioelectron 22:3146–3153
14. Liu Y, Wang MK, Zhao F, Xu ZA, Dong SJ (2005) Biosens Bioelectron 21:984–988
15. Liu Q, Lu XB, Li J, Yao X, Li JH (2007) Biosens Bioelectron 22: 3203–3209
16. Salimi A, Compton RJ, Hallaj R (2004) Anal Biochem 333: 49–56
17. Deng CY, Chen JH, Chen XL, Xiao CH, Nie L, Yao SZ (2008) Biosens Bioelectron 23:1272–1277
18. Shan D, Wang SX, Xue HG, Cosnier S (2007) Electrochem Commun 9:529–534
19. Zhou GJ, Wang G, Xu JJ, Chen HY (2002) Sens Actuators B 81: 334–339
20. Åsberg P, Inganäs O (2003) Biosens Bioelectron 19:199–207
21. Pan LJ, Yu GH, Zhai DY, Lee HR, Zhao WT, Liu N, Wang HL, Tee BCK, Shi Y, Cui Y, Bao ZA (2012) Proc Natl Acad Sci U S A 109: 9287–9292
22. Zhai DY, Liu BR, Shi Y, Pan LJ, Wang YQ, Li WB, Zhang R, Yu GH (2013) ACS Nano 7:3540–3546
23. Zhou GM, Wang DW, Li F, Zhang LL, Weng Z, Cheng HM (2011) New Carbon Mater 26:180–186
24. Zhou Y, Qin ZY, Li L, Zhang Y, Wei YL, Wang LF, Zhu MF (2010) Electrochim Acta 55:3904–3908
25. Lai C, Zhang HZ, Li GR, Gao XP (2011) J Power Sources 196:4735–4740
26. Ali HG, Ikhlas AM, Ahmed BZ, Rehab GEl-S (2008) Appl Catal B Environ 80:106–115

27. Sheng QL, Wang MZ, Zheng JB (2011) Sens Actuat B 160:1070–1077
28. Wang MZ, Sheng QL, Zhang DW, He YP, Zheng JB (2012) Bioelectrochemistry 86:46–53
29. Ou YW, Cui XL, Zhang XY, Jiang ZY (2010) J Power Sources 195: 1365–1369
30. Zhao YF, Wang W, Xiong DB, Shao GJ, Xia W, Yu SX, Gao FM (2011) Int J Hydrogen Energ. doi:10.1016/j.ijhydene.2011.09.123
31. Vankayala K, Suresh BK, Balaji RJ, Srinivasan S (2011) Electrochim Acta 56:10493–10499
32. Alicja S, Antonio RS, Benjamin H, Bastian JME, Thomas TUK (2012) J Power Sources 199:22–28
33. Ma JH, Wu MN, Du YH, Chen SQ, Li GX, Hu JB (2008) Mat Sci Eng B 153:96–99
34. Zeng ZY, Tu JP, Huang XH, Wang XL, Xiang JY (2009) Thin Solid Films 517:4767–4771
35. Ranjan D, John C, Gleb Y, Yury G, Giovanna L, Jonathan S, John F, Sergei K (2006) Carbon 44:2489–2497
36. Ehret R, Baumann W, Brischwein M, Schwinde A, Stegbauer K, Wolf B (1997) Biosens Bioelectron 12:29–41
37. Liu XJ, Huang YX, Zhang WJ, Fan GF, Fan CH, Li GX (2005) Langmuir 21:375–378
38. Laviron E (1979) J Electroanal Chem 101:19–28
39. Hasegawa K, Kimura A, Yamamura T, Shiokawa Y (2005) J Phys Chem Solids 66:593–595
40. Sun W, Li XQ, Wang Y, Li X, Zhao CZ, Jiao K (2009) Bioelectrochemistry 75:170–175
41. Wu YH, Shen QC, Hu SS (2006) Anal Chim Acta 558:179–186
42. Gao RF, Zheng JB (2009) Electrochem Commun 11:1527–1529
43. Jun H, Hedayatollah G, Moosavi-Movahedi AA (2006) Electrochem Commun 8:1572–1576
44. Miao X, Liu Y, Gao WC, Hu NF (2010) Bioelectrochemistry 79:187–192
45. Qiu JD, Peng HP, Liang RP, Xia XH (2010) Biosens Bioelectron 25: 1447–1453
46. Zhang L, Tian DB, Zhu JJ (2008) Bioelectrochemistry 74:157–163
47. Qiao K, Hu NF (2009) Bioelectrochemistry 75:71–76
48. Kamin RA, Wilson GS (1980) Anal Chem 52:1198–1205
49. Shu FR, Wilson GS (1976) Anal Chem 48:1679–1686
50. Wang Y, Qian WP, Tan Y, Ding SH, Zhang HQ (2007) Talanta 72: 1134–1140
51. Huang KJ, Sun JY, Jin CX, Jing QS, Zhou T (2011) Thin Solid Films 519:3925–3930
52. Yang WY, Zhou X, Zheng N, Li XJ, Yuan ZB (2011) Electrochim Acta 56:6588–6592
53. Salimi A, Hallaj R, Soltanian S (2007) Biophys Chem 130:122–131
54. Zhang GH, Yang NB, Ni YL, Shen J, Zhao WB, Huang XH (2011) Sens Actuators B 158:130–137
55. Huang KJ, Sun JY, Niu DJ, Xie WZ, Wang W (2010) Colloid Surface B 78:69–74
56. Ding Y, Wang Y, Lei Y (2010) Biosens Bioelectron 26:390–397
57. Dong SY, Zhang PH, Liu H, Li N, Huang TL (2011) Biosens Bioelectron 26:4082–4087
58. Ma W, Tian DB (2010) Bioelectrochemistry 78:106–112
59. Bard AJ, Faulkner LR (1980) Electrochemical Methods. John Wiley & Sons, New York